Heliyon 10 (2024) e23520

Contents lists available at ScienceDirect

Heliyon

journal homepage: www.cell.com/heliyon

Establishment of a novel overlay culture method that enables immune response assessment using gastric cancer organoids

Hiroshi Ota [a], Kazuaki Tanabe [b,*], Yoshihiro Saeki [a,c], Yuki Takemoto [a], Emi Chikuie [a], Naoya Sakamoto [d], Hideki Ohdan [a]

[a] *Department of Gastroenterological and Transplant Surgery, Applied Life Sciences, Institute of Biomedical & Health Science, Hiroshima University, 1-2-3 Kasumi Minami-ku, Hiroshima, 734-8551, Japan*

[b] *Department of Perioperative and Critical Care Management, Graduate School of Biomedical and Health Sciences, Hiroshima University, 1-2-3 Kasumi Minami-ku, Hiroshima, 734-8551, Japan*

[c] *Division of Endoscopic Surgery, Hofu Institute of Gastroenterology, Hiroshima University Hospital, 14-33 Ekiminami-machi, Yamaguchi, 747-0801, Japan*

[d] *Department of Molecular Pathology, Graduate School of Biomedical and Health Sciences, Hiroshima University, 1-2-3 Kasumi, Minami-ku, Hiroshima, 734-8551, Japan*

ARTICLE INFO

Keywords:
Organoids
Gastric cancer
Immunotherapy
Peripheral blood mononuclear cells
Natural killer cells

ABSTRACT

Organoid technology, a novel 3D cell culture system, can reproduce a patient's cancer and may be a novel immunotherapy experimental model. However, currently no gastric cancer organoid (GCO) models in which the organoid and immune cells are in free contact and sufficiently react with each other exist. In this study, we aimed to create a coculture model in which immune cells can move freely and stay in contact with GCOs. We coated the bottom surface of the plate with Matrigel and adhered stem cells to the Matrigel surface, instead of completely embedding them in Matrigel to culture organoids. This method allowed GCOs to grow on the Matrigel surface while maintaining a three-dimensional structure and reproducing the characteristics of the patient's cancer. We cocultured GCOs and immune cells. Using this model, immune cells could freely move and were in sufficient contact with the cultured GCOs. Our model allowed real-time observation of the immune response and tumor destruction with time. In addition, the GCO killing assay was assessed with natural killer cells from the same patient. This organoid culture model enabled repeated evaluation of the GCO killing assay with various immune cells *in vitro*. We established a new experimental model that allowed free movement of immune cells and sufficient contact with GCOs. Using this model, it may be possible to predict the effects of immune checkpoint inhibitors *in vitro* (using GCOs) before administering them to patients.

1. Introduction

Gastric cancer (GC) is the fourth leading cause of cancer-related deaths, accounting for approximately 780,000 deaths each year worldwide [1]. Although survival has gradually improved with the development of chemotherapy and immune checkpoint inhibitors such as the anti-programmed cell death-1 (PD-1) antibody [2], the overall survival is still 13.8 months even with chemotherapy and nivolumab administration [3]. Therefore, further research is required to identify better treatment options for advanced GC. As a

* Corresponding author.
E-mail address: ktanabe2@hiroshima-u.ac.jp (K. Tanabe).

https://doi.org/10.1016/j.heliyon.2023.e23520
Received 18 January 2023; Received in revised form 19 November 2023; Accepted 5 December 2023
Available online 9 December 2023

project of The Cancer Genome Atlas (TCGA), a comprehensive analysis of molecular abnormalities in GC was conducted and four new molecular subtypes (1, Epstein-Barr virus; 2, microsatellite instability; 3, genomically stable, and 4, chromosomal instability) were proposed [4]. These molecular subtypes are expected to serve as a roadmap for patient stratification and clinical trials using molecular-targeted therapies. Furthermore, clinical trials using immune checkpoint inhibitors are underway [3,5]. These studies have analyzed the expression rate of programmed cell death 1- ligand 1 (PDL-1), PDL-1 combined positive score, and microsatellite instability (MSI) to predict the effect of immune checkpoint inhibitors [2,3,5–7]. Such studies are often conducted using histopathological examination on surgical specimens. Although cancer cell lines are used in *in vitro* experiments, they do not completely reproduce the properties of the cancer environment in patients. Thus, organoids, with an ability to three-dimensionally reproduce cancers derived from patients, are attracting attention as a novel cancer model. The model has currently been applied to several types of cancer tissues including GC [8–17], and it has been confirmed that cancer organoids reproduce most genetic and histological features of the parental tumor from which they are derived [15].

We have reported the establishment of anticancer drug-resistant GC organoids (GCOs) and the identification of molecules that acquire 5-fluorouracil (5-FU) and oxaliplatin resistance [18,19]. In addition, the model is expected to be useful to investigate the reaction between cancer and immune cells *in vitro* through coculturing cancer organoids and immune cells. In the conventional method of organoid culture, organoids are embedded in an extracellular matrix such as Matrigel until they grow, and then, immune cells are added to the outside of the extracellular matrix to react with the organoid, which does not sufficiently invade the Matrigel. Cancer organoids derived from patients are repeatedly separated into single cells and cocultured with T cells to create strong chimeric antigen receptor–T-cell (CAR-T), which damages cancer organoids [20]. However, the killing assay reported in this study involves the coculture of organoids and immune cells without the extracellular matrix, which is conventionally required to culture organoids. Therefore, the survival environment in this model is different from that in the conventional method in which organoids are embedded in the extracellular matrix. It is possible that the length of survival of the organoids cultured without the extracellular matrix may be different from that of organoids in the normal culture at the time of coculture, and the immune response may also change.

Currently, there are no GCO models in which the organoid and immune cells are in free contact and react sufficiently with each other. Therefore, the aim of this study was to create a coculture model in which immune cells can move freely and have sufficient contact with GCOs.

2. Material and methods

2.1. Human tissues

Human GC and normal gastric tissues were obtained from patients who underwent surgery at the Department of Gastroenterological and Transplant Surgery at Hiroshima University Hospital. Clinical data of the patient-derived organoids are summarized in Supplementary Table 1. Tumor staging was determined according to the TNM classification system. The histological classifications were determined based on the guidelines of the Japanese Research Society for Gastric Cancer [21]. Written informed consent for the establishment of the organoids was obtained from the patients. This study was approved by the Ethics Committee for Human Genome Research of Hiroshima University, Hiroshima (E-597-01 and E-1789-1) and was conducted in accordance with the Ethical Guidance for Human Genome/Gene Research of the Japanese Government.

2.2. Establishment and culture of human GC organoids

Human GCOs were established and cultured in organoid media containing the niche factors described previously [18] and were passaged twice a week with a split ratio of 1:3/1:6. The culture method used under these conditions is referred to as the conventional culture method (CCM).

2.3. Establishment and culture of human GCOs using the overlay culture method

The bottom of a 48-well plate was coated with 100 μL Matrigel per well. Human GCOs were separated into single cells using TrypLE™ express (Thermo Fisher, Waltham, MA, USA) and 1×10 [4] cells per well were seeded; then, 200 μL Matrigel per well was added to the bottom of the well. The human GCOs were maintained as described previously [18] in a humidified atmosphere of 5% CO_2 and 95% air at 37 °C. The culture method under these conditions is referred to as the overlay culture method (OCM).

2.4. Immunohistochemistry and scoring

Immunohistochemical analysis was performed with a Dako Envision + Mouse/Rabbit Peroxidase Detection System (Dako Cytomation, Carpinteria, CA, USA). Antigen retrieval was performed using a pressure cooker heated to 100 °C in citrate buffer (pH 6.0) for 5 min. Peroxidase activity was blocked with 3% H_2O_2-methanol for 10 min.

Sections were incubated with anti-MUC5AC (anti-MRQ-19, 760-4389, V0001348, Roche; 1:2 dilution for IHC), anti-MUC6 (NCL-MUC-6, 6014968, Leica Biosystems; 1:100 dilution for IHC), anti-MUC2 (anti-MRQ-18, 760-4388, V0001436, Roche; 1:2 dilution for IHC), anti-CD10 (56C6, CD10-270, 602420, Leica Biosystems; 1:100 dilution for IHC), or anti-Ki67 (NCL-L-Ki67-MM1, Leica Biosystems; 1:100 dilution for IHC) antibodies for 1 h at 25 °C, followed by incubation with Envision and the anti-mouse peroxidase for 1 h at room temperature. For color reactions, sections were incubated with DAB substrate-chromogen solution (Dako Cytomation) for 5

min. Sections were counterstained with 0.1% hematoxylin & eosin. Reactions lacking a primary antibody were used as negative controls.

2.5. Microarray

Total RNA was isolated from human GCOs with the RNeasy mini kit (Qiagen, Hilden, German). RNA integrity was assessed with an Agilent 2100 Bioanalyzer (Agilent Technologies, Santa Clara, CA, USA). The total RNA extracted (100 ng, RIN $>$ 6) was converted to single-strand cDNA using a GeneChip™ WT PLUS Reagent Kit (Thermo Fisher, Waltham, MA, USA). Hybridization was performed using the Clariom S Array, human (Thermo Fisher) in an Affymetrix GeneChip Hybridization Oven 645 (Affymetrix, USA). After washing and staining, the probe arrays were scanned using an Affymetrix GeneChip Scanner 3000 7G. GCO RNAs were analyzed in both cultures using a microarray. After averaging the RNAs of both groups, we searched for genes with a $\geq$2-fold difference in the expression level and an unpaired *t*-test p value of $<$0.05.

2.6. Human peripheral blood cells isolation

Blood was collected from all participants, and the peripheral blood mononuclear cells (PBMCs) were isolated using gradient centrifugation with Lympholyte-H (Cedarlane, Canada). For the immune cell infiltration assay, PBMCs were labeled with 5 μM 5-(and 6)-carboxyfluorescein succinimidyl ester (CFSE) (Thermo Fisher Scientific). Written informed consent for collecting the patients' blood was obtained from all patients. This study was approved by the Ethics Committee for Human Genome Research of Hiroshima University, Hiroshima (E-597-01 and E-1789-1) and was conducted in accordance with the Ethical Guidance for Human Genome/Gene Research of the Japanese Government.

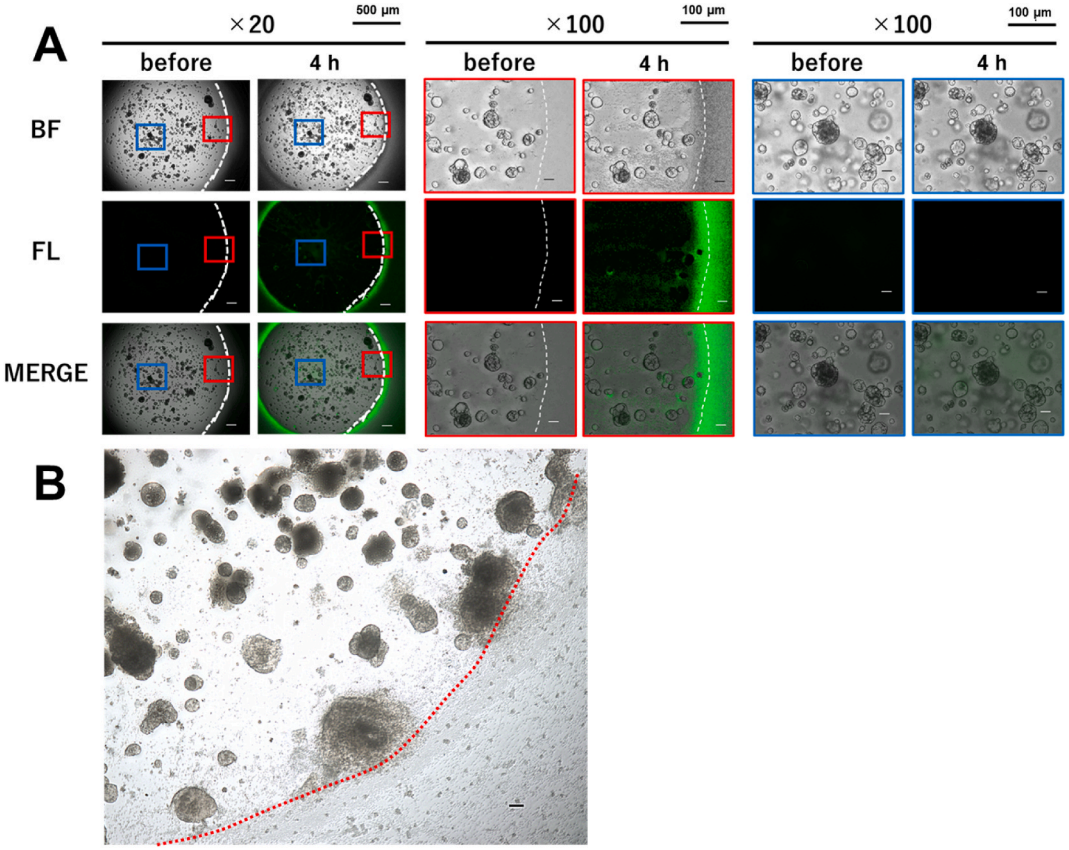

Fig. 1. Coculture of immune cells and gastric cancer organoid (GCOs) using the conventional culture method. (A) Images of coculture of immune cells stained with CFSE and conventional GCOs (original magnification 20×, left and 100×, center and right, scale bar: 500 μm, left and 100 μm, center and right). Upper: bright field. Central: fluorescence. Lower: merge. (B) Images of coculture of immune cells and conventional GCOs (original magnification 100×, scale bar: 100 μm). The dotted line is the boundary of the Matrigel.

2.7. Human natural killer cell isolation

Human PBMCs were separated into natural killer (NK) and non-NK cell fractions using the Human NK Cell Isolation kit II (Miltenyi Biotec). Extracted cells were analyzed through flow cytometry (BD FACSCanto II), and only samples with more than 90% purity of

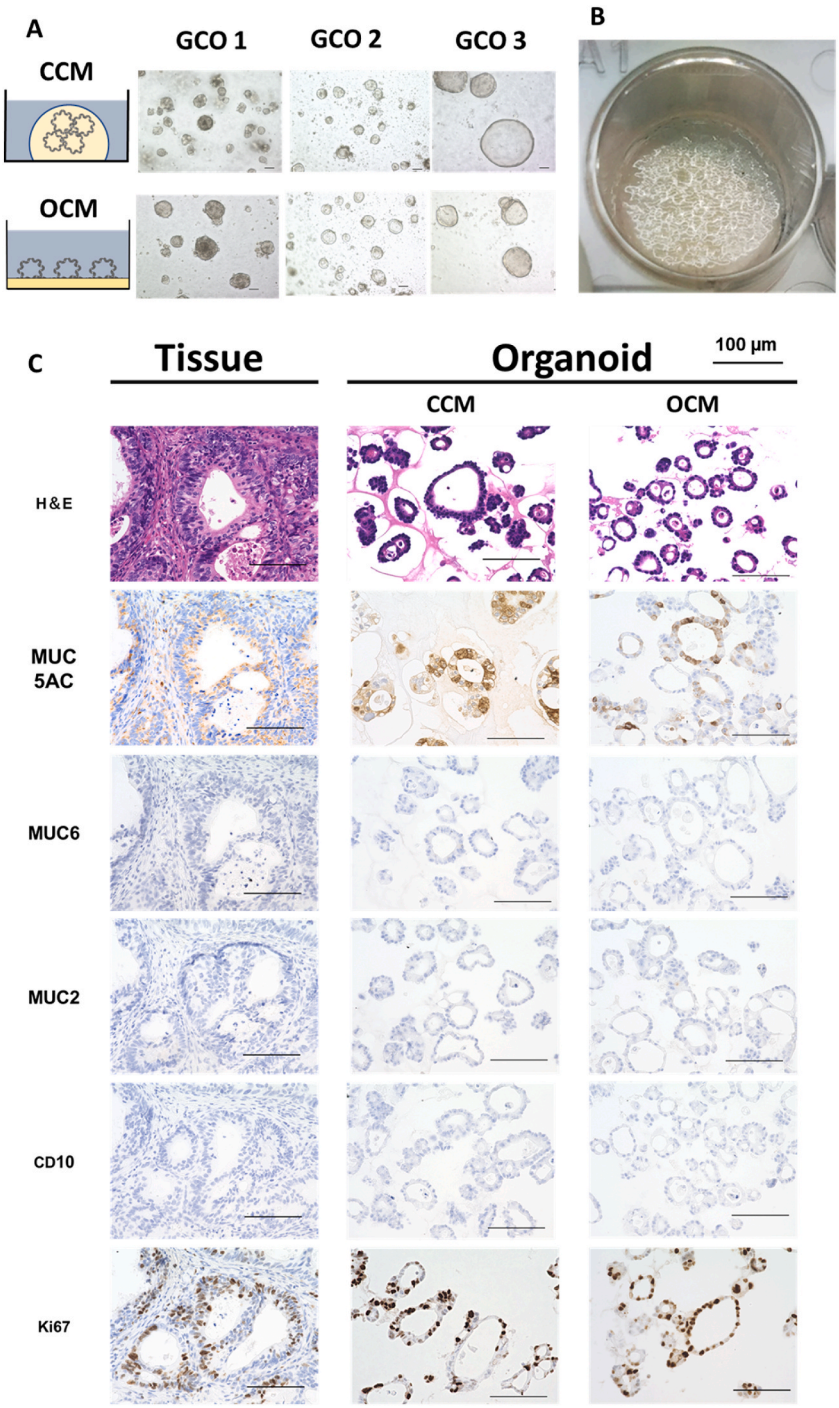

Fig. 2. GCOs grown three-dimensionally using the overlay culture method. (A) Representative images of GCOs from the overlay culture method (original magnification 100×, scale bar: 100 μm). Upper: conventional culture method (CCM), lower: overlay culture method (OCM). (B) A representative photograph of GCOs grown three-dimensionally using the overlay culture method. (C) Representative images of immunohistochemical staining and H&E staining of GCO1 (original magnification 400×, scale bar: 100 μm) Left: primary tissue, center: GCOs by CCM, right: GCOs using the OCM).

isolated fractions were used for cytotoxicity tests.

2.8. GCO killing assay

The GCO killing assay was assessed with a standard methyl thiazolyl tetrazolium (MTT) assay, which detects dehydrogenase activity in viable cells. In brief, 5×10^5 PBMCs or NK cells were seeded in each well of 48-well culture plates with human GCOs and cocultured. After 24 h, the culture medium was removed, and 50 μL of a 0.5 mg/mL solution of MTT (Sigma-Aldrich) was added to each well. The plates were then incubated for 1 h at 37 °C. The MTT solution was then removed and replaced with 50 μL dimethyl sulfoxide (DMSO; Wako, Osaka, Japan) per well, and the absorbance at 570 nm was measured using an MTP-310 microplate reader (CORONA electric, Ibaraki, JAPAN). Before adding DMSO, the Matrigel was dissolved in 100 μL of 2% SDS (Wako, Osaka, Japan). Coculture experiments were conducted with NK cells using concanamycin A (Fujifilm Wako Pure Chemical Corporation, Osaka, Japan), which specifically inhibits the perforin-dependent pathway.

2.9. Statistical analysis

Statistical differences were evaluated using the Student's *t*-test for 2 groups, or Tukey HSD test for 3 groups. The results are expressed as the mean ± standard deviation of triplicate measurements. We considered $p < 0.05$ to be statistically significant.

3. Results

3.1. Establishment of GCOs using the OCM

In the CCM, immune cells stained with CFSE invaded the vicinity of the Matrigel boundary but did not invade the center of the Matrigel (Fig. 1a). Although GCO tissue destruction was observed near the boundary of the Matrigel invaded by immune cells, it was not observed for tissues located deep inside the Matrigel (Fig. 1b). Therefore, we coated the bottom surface of the plate to be cultured with Matrigel and adhered stem cells to its surface (Supplementary Fig. 1). After two weeks, the GCOs grown using this method presented the same morphology as those in the CCM (Fig. 2a) and irregularities were observed on the surface of Matrigel, which implies that the three-dimensional structure was reconstructed even in the unembedded part (Fig. 2b). In addition, hematoxylin and eosin (H&E) staining revealed that the GCOs in this culture method showed the same tissue type as the tumor tissue and the GCOs in the CCM. Immunostaining revealed that same properties were also maintained (Fig. 2c, Supplementary Fig. 2).

3.2. Microarray analysis of the OCM GCOs

We performed a microarray analysis to examine whether the GCOs from the OCM and those from the CCM maintained the same properties. GCO RNAs (17,834) were analyzed in both cultures using a microarray. After averaging the RNAs of both groups, we searched for genes with a difference in the expression level of ≥2 and unpaired *t*-test $p < 0.05$. Only 16 RNAs met this criteria, and 99.91% (17,818/17,834) of RNA expression levels were similar in both groups (Fig. 3).

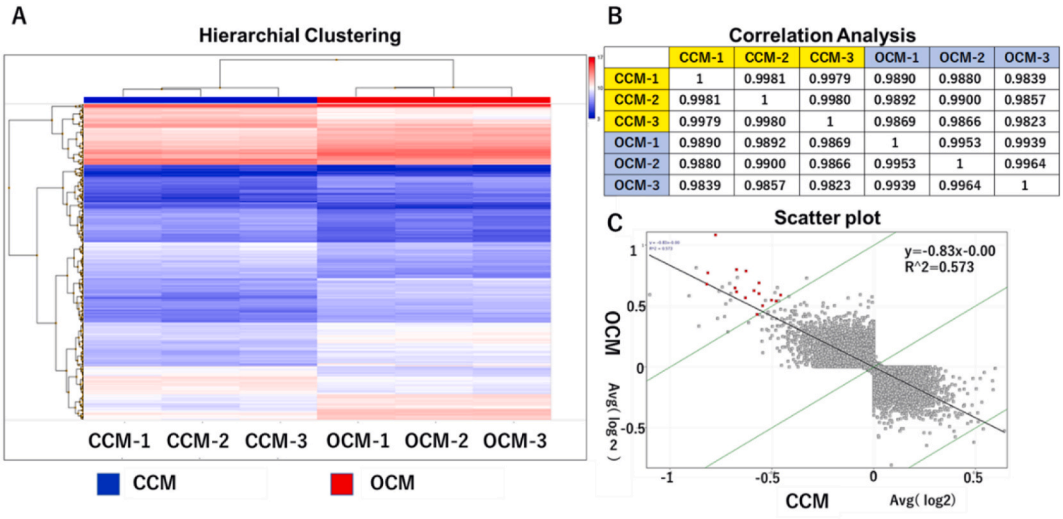

	CCM-1	CCM-2	CCM-3	OCM-1	OCM-2	OCM-3
CCM-1	1	0.9981	0.9979	0.9890	0.9880	0.9839
CCM-2	0.9981	1	0.9980	0.9892	0.9900	0.9857
CCM-3	0.9979	0.9980	1	0.9869	0.9866	0.9823
OCM-1	0.9890	0.9892	0.9869	1	0.9953	0.9939
OCM-2	0.9880	0.9900	0.9866	0.9953	1	0.9964
OCM-3	0.9839	0.9857	0.9823	0.9939	0.9964	1

Fig. 3. ray analysis of GCOs through CCM or OCM. (A) Hierarchical clustering of microarray analysis of GCOs with CCM or OCM. (B) Correlation analysis between GCOs and CCM or OCM. (C) The red dots are genes with a fold change difference of ≥2 (expression level difference was more than double) and unpaired Students *t*-test $p < 0.05$.

3.3. Immune cell infiltration assay using the overlay GCO culture model

To confirm that immune cells can freely contact GCOs in this OCM, we cocultured GCOs with CFSE-stained healthy donor PBMCs. Four hours after coculture, PBMCs aggregated around almost all GCOs, and confirmed that immune cells could freely move and contact with GCOs (Fig. 4).

3.4. Overlay GCO killing assay with PBMCs from healthy donors

To determine whether this culture method causes tissue destruction by immune cells and to evaluate the degree of destruction, GCOs grown using the OCM and PBMCs obtained from healthy donors were cocultured for 20 h. Microscopic images showed GCO tissue destruction in the coculture group. The MTT assay showed that PBMC destroyed 66.1% of GCO tissue in case 2 and 53.6% of GCOs in case 3 (Fig. 5a and b). Furthermore, we could capture the movement of PBMCs moving freely and destroying GCOs in real time (Supplementary Fig. 3).

3.5. Overlay GCO killing assay with NK cells from healthy donors

To simplify the experimental model and selectively analyze the response of NK cells alone (and not that of all immune cells), the OCM GCO tissue destruction assay was performed in coculture with NK cells. NK cells were isolated from PBMCs from healthy subjects, and GCO and NK cells were cocultured using the same protocol as the one previously described. In addition, to confirm that tissue destruction was caused by NK cells, concanamycin A(Fujifilm Wako Pure Chemical Corporation, Osaka, Japan), which specifically inhibits the perforin-dependent pathway, which is one of the cytotoxic pathways of NK cells, was used. Experiments were conducted in three groups: non-coculture (control group), NK cell and GCO coculture group, and NK cell and GCO coculture group with the addition of concanamycin A. Microscopic images showed GCO tissue destruction in the NK cell coculture group compared with that in the control group. Tissue destruction was suppressed in the concanamycin A group (Fig. 6a). In addition, the MTT assay showed 77.1% tissue destruction in the NK cell coculture group but only 55.1% in the concanamycin A group; therefore, tissue destruction was significantly suppressed ($p < 0.01$) (Fig. 6b). We revealed the movement of NK cells that destroy GCO in time lapse (Supplementary Fig. 4). From these results, we confirm GCO tissue destruction by NK cells using the OCM GCOs and NK cell coculture.

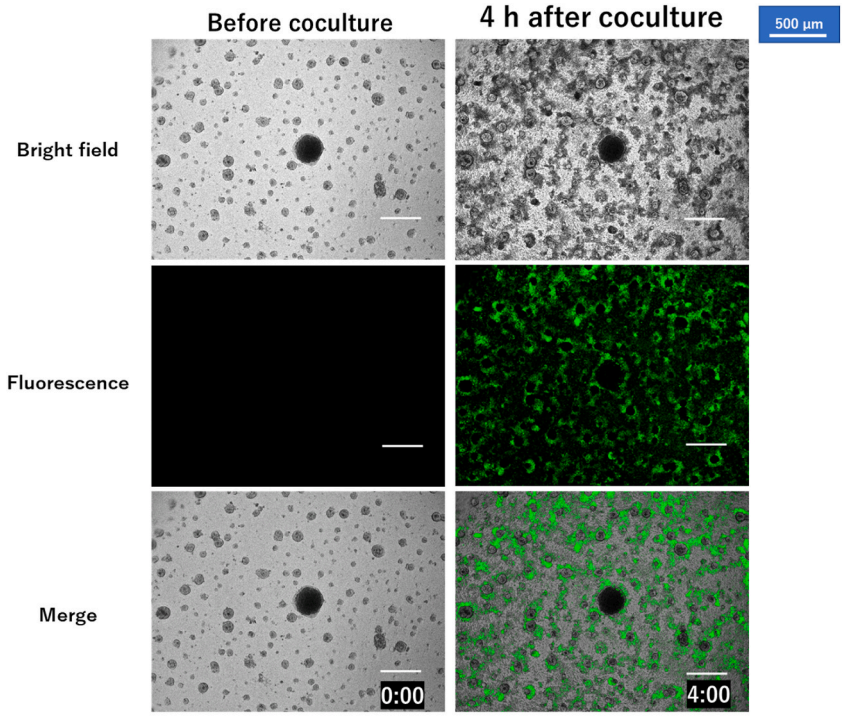

Fig. 4. Coculture of immune cells and GCOs using the overlay culture method. Representative images of GCOs obtained using the overlay culture method (original magnification 100×, scale bar: 500 μm). Upper: bright field. Central: fluorescence. Lower: merge. Lower numbers represent elapsed time.

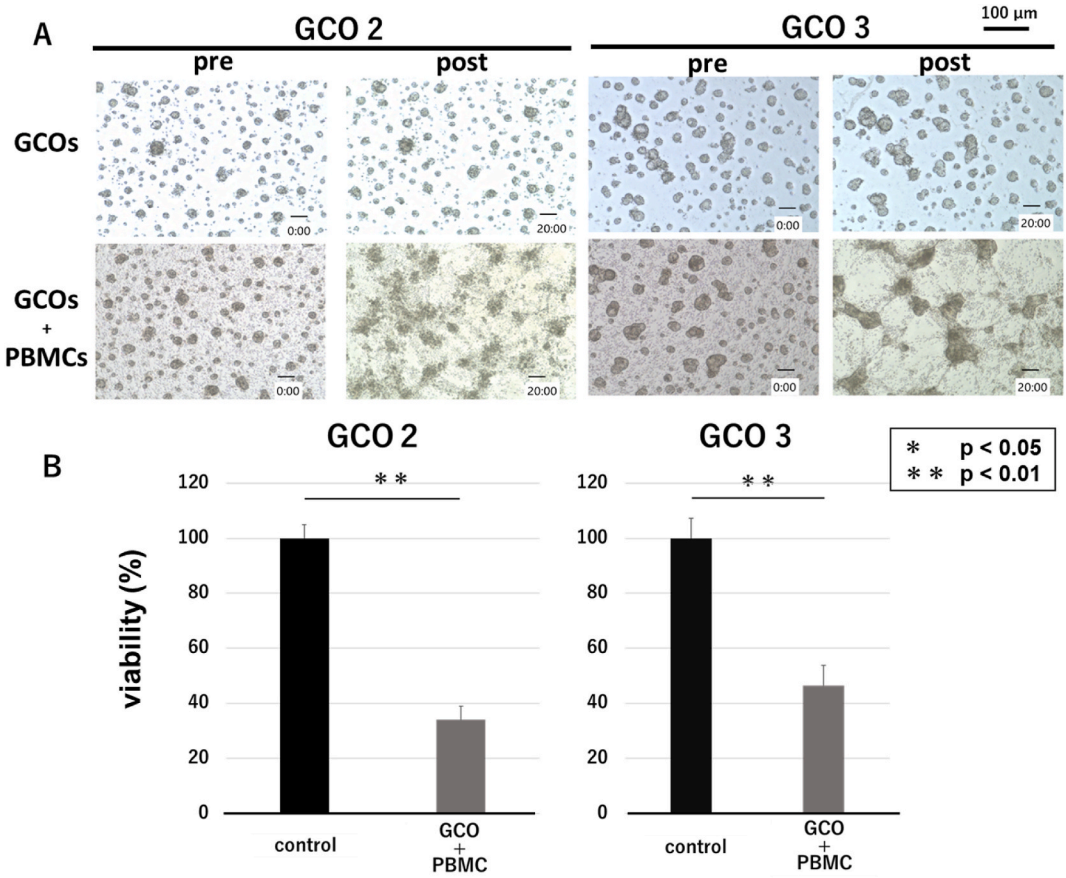

Fig. 5. Overlay GCO killing assay using PBMCs from a healthy donor. (A) Representative images of GCOs using the overlay culture method (original magnification 100×, scale bar: 100 μm). Upper: GCOs only. Lower: coculture of GCOs and PBMCs from a healthy donor. Left: before coculture. Right: after coculture. Lower numbers indicate elapsed time. (B) Overlay GCO killing assay using PBMCs from a healthy donor.

3.6. Overlay GCO killing assay with patient-derived NK cells

Patient-derived GCOs and NK cells extracted from the same patient-derived PBMCs were cocultured, and the same assay was conducted (Fig. 7a). Microscopic images showed GCO tissue destruction in the NK cell coculture group compared with that in the control group, and tissue destruction was suppressed in the concanamycin A group (Fig. 7b). In addition, the MTT assay also showed that 91.6% of the tissues were destroyed in case 2 and 56.3% in case 3. Tissue destruction was significantly suppressed in the concanamycin A group ($p < 0.05$) (Fig. 7c). We demonstrated the movement of patient-derived NK cells that destroyed GCO in time lapse (Supplementary Fig. 5). This experiment demonstrated that patient-derived NK cells can be used to assess the degree of tissue destruction against patient GCOs.

4. Discussion

We established an experimental model in which almost all organoids in the observation range are in contact with immune cells using an overlay culture. In the conventional organoid culture method, the Matrigel interferes with experimental models such as the anticancer drug susceptibility test and tailor-made treatment using immune cells.

Nakano et al. grew optic cup organoids without complete embedding by adding 1% Matrigel to the medium [22]. We used an approach similar to that of Nakano et al. and instead of completely embedding organoids in Matrigel, which is necessary for culturing organoids, we coated the bottom surface of the plate in which organoids were to be cultured with Matrigel, and adhered stem cells to its surface. This method allowed organoids to grow on the surface of the Matrigel while maintaining a three-dimensional structure and allowing immune cells to freely contact the organoids. In addition, our experimental model allows real-time observation of the immune response and tumor destruction.

To reveal that this model can be used to evaluate tumor damage, we cocultured patient-derived GCOs and healthy donor-derived PBMCs. We demonstrated the destruction of organoids by PBMC through imaging, time lapse, and the MTT assay. Next, to simplify the experimental model, NK cells were purified from PBMCs, and similar experiments were performed; we demonstrated the destruction of

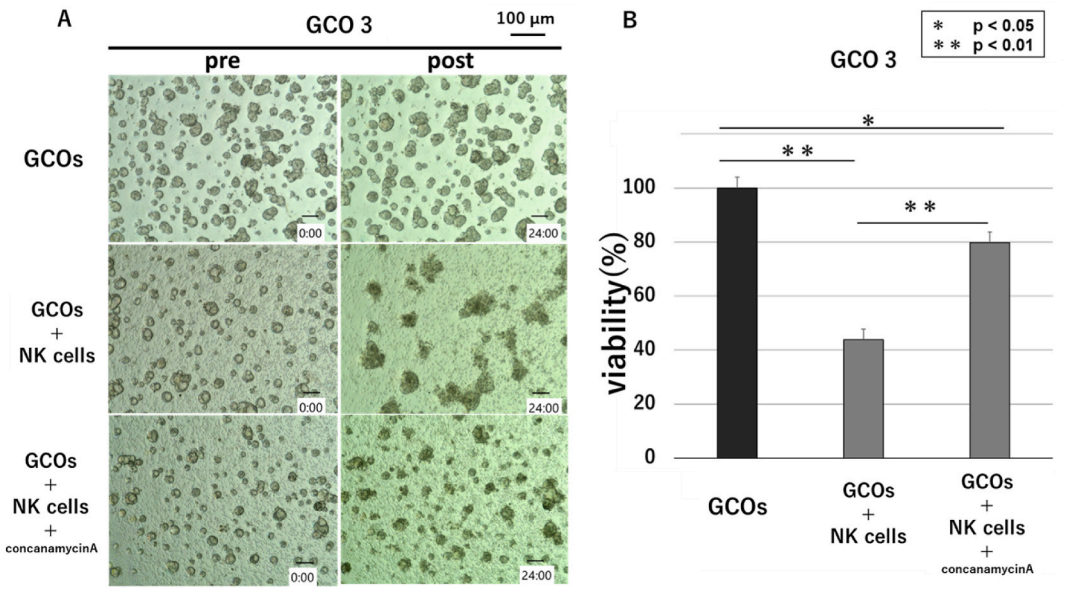

Fig. 6. Overlay GCO killing assay using NK cells of a healthy donor. (A) Representative images of GCOs using the overlay culture method (original magnification 100×, scale bar: 100 μm). Upper: GCOs only. Central: coculture of GCOs and NK cells from a healthy donor. Lower: coculture of GCOs and NK cells from a healthy donor with the addition of concanamycin A. Left: before coculture. Right: after coculture. Lower numbers represent elapsed time. (B) Overlay GCO killing assay using NK cells of a healthy donor.

GCOs with NK cells as well. Furthermore, we obtained similar results for coculture patient-derived NK cells and same-patient-derived GCOs. These results showed that our culture method allows the organoids to come into free contact with immune cells and generate an immune response and is useful to evaluate tumor destruction.

Krijn et al. reported the establishment of tumor-specific T cells through coculturing immune cells with single-celled cancer organoids. Furthermore, they demonstrated that T cells show tumor-specific injury by coculturing the T cells with cancer organoids [20]. The major difference between their and our study is that they digested the extracellular matrix around organoids when coculturing immune cells and organoids and we did not. By culturing the organoids on the surface of the extracellular matrix, we ensured sufficient contact of the organoids with immune cells while the organoids were still alive. As a result, organoids that normally die when the extracellular matrix is digested, were found to be alive, which may enable their observation for a longer period of time. In addition, we confirmed that GCOs grown using this method maintained not only the properties of GCOs from the normal culture method but also the same morphology and properties as the cancer tissue of the patient. Thus, by extracting immune cells from the blood of the patient who established GCOs and ensuring contact with GCOs, the reaction between cancer and immune cells *in vivo* was observed and analyzed *in vitro*. In addition, we demonstrated that GCOs and patient-derived NK cells can be cocultured to perform the GCO killing assay. Using this experimental model and adding an immune checkpoint inhibitor to the coculture of GCOs and patient's immune cells in the OCM, it will be possible in the future to evaluate the predictive effect on the patient before administration of the immune checkpoint inhibitor *in vitro*.

In various types of cancers, immunotherapy and immunochemotherapy are gaining attention because of recent advances in immunotherapy. However, since this study only examined gastric cancer, it is necessary to perform studies on other cancers in the future. In addition, the model analyzed in this study used only co-culture with NK cells, but coculture must be performed with other lymphocytes including T cells.

Funding

This study was supported by Grants-in-Aid for Scientific Research (JP19H01057, JP21K08734, JP17K10591) from the Japan Society for the Promotion of Science.

Data availability statement

Data associated with the study has not been deposited into a publicly available repository and data will be made available on request.

CRediT authorship contribution statement

Hiroshi Ota: Writing – original draft, Investigation, Formal analysis, Data curation. **Kazuaki Tanabe:** Writing – review & editing,

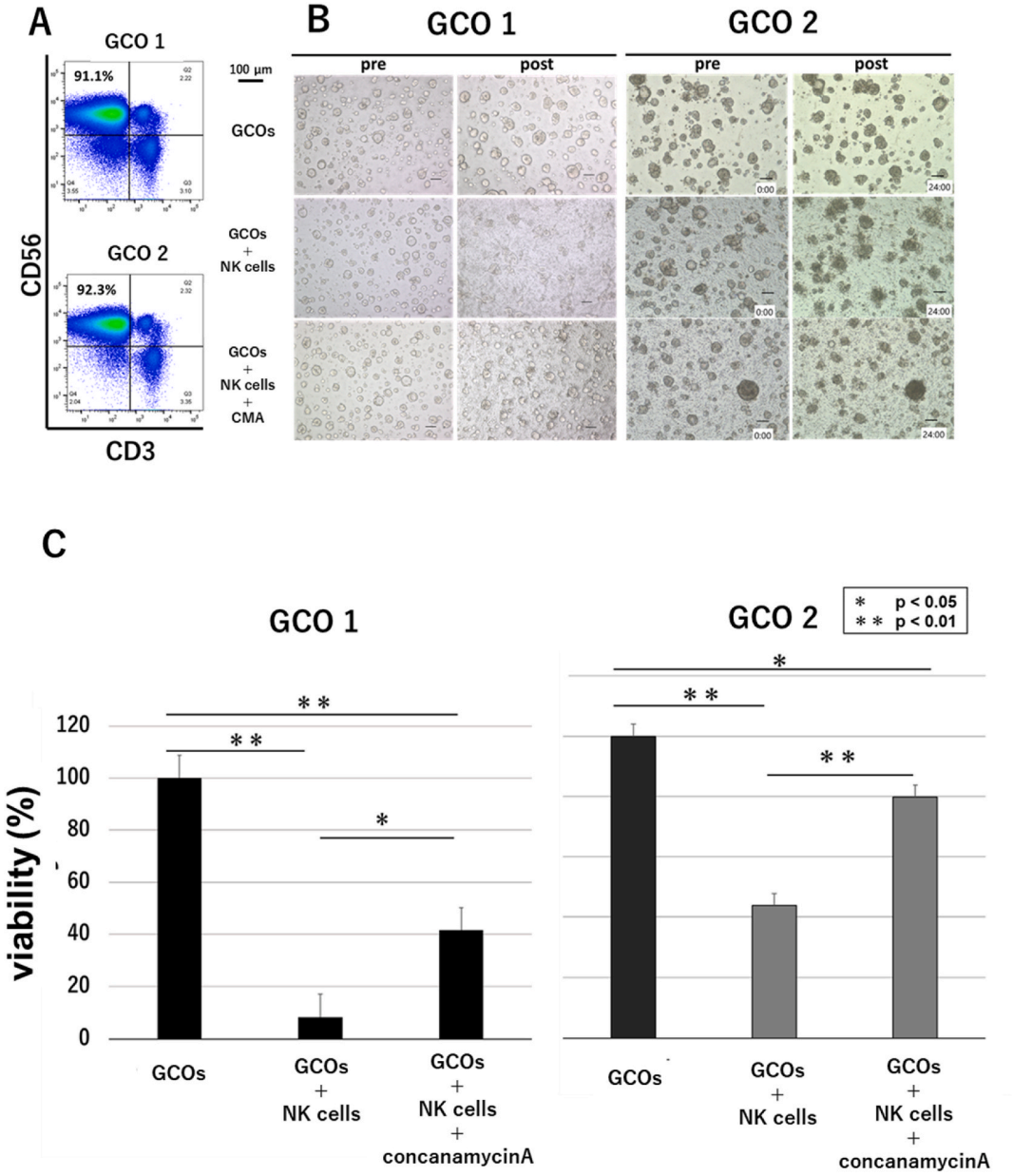

Fig. 7. Overlay GCO killing assay using patient-derived NK cells. (A) Analysis of NK cell purity using flow cytometry. (B) Representative images of GCOs using the overlay culture method (original magnification 100×, scale bar: 100 μm). Upper: GCOs only. Central: coculture of GCOs and patient-derived NK cells. Lower: coculture of GCOs and patient-derived NK cells with the addition of concanamycin A. Left: before coculture. Right: after Coculture. Lower numbers represent elapsed time. (C) Overlay GCO killing assay using patient-derived NK cells.

Supervision, Funding acquisition. **Yoshihiro Saeki:** Project administration, Data curation. **Yuki Takemoto:** Validation, Investigation. **Emi Chikuie:** Investigation. **Naoya Sakamoto:** Validation, Methodology. **Hideki Ohdan:** Supervision, Funding acquisition, Conceptualization.

Declaration of competing interest

The authors declare that they have no known competing financial interests or personal relationships that could have appeared to influence the work reported in this paper.

Acknowledgements

We thank the Analysis Center of Life Science of Hiroshima University for the use of their facilities. The R-spondin-producing cell line was a kind gift from Prof. Jeffery Whitsett (Cincinnati Children's Hospital Medical Center, Cincinnati, OH, USA).

Appendix A. Supplementary data

Supplementary data to this article can be found online at https://doi.org/10.1016/j.heliyon.2023.e23520.

References

[1] F. Bray, J. Ferlay, I. Soerjomataram, R.L. Siegel, L.A. Torre, A. Jemal, Global cancer statistics 2018: GLOBOCAN estimates of incidence and mortality worldwide for 36 cancers in 185 countries, CA A Cancer J. Clin. 68 (2018) 394–424.
[2] Y.K. Kang, N. Boku, T. Satoh, M.H. Ryu, Y. Chao, K. Kato, et al., Nivolumab in patients with advanced gastric or gastro-oesophageal junction cancer refractory to, or intolerant of, at least two previous chemotherapy regimens (ONO-4538-12, ATTRACTION-2): a randomised, double-blind, placebo-controlled, phase 3 trial, Lancet 390 (2017) 2461–2471.
[3] Y.Y. Janjigian, K. Shitara, M. Moehler, M. Garrido, P. Salman, L. Shen, et al., First-line nivolumab plus chemotherapy versus chemotherapy alone for advanced gastric, gastro-oesophageal junction, and oesophageal adenocarcinoma (CheckMate 649): a randomised, open-label, phase 3 trial, Lancet 398 (2021) 27–40.
[4] Cancer Genome Atlas Research Network, Comprehensive molecular characterization of gastric adenocarcinoma, Nature 513 (2014) 202–209.
[5] Y.K. Kang, L.T. Chen, M.H. Ryu, D.-Y. Oh, S.C. Oh, H.C. Chung, et al., Nivolumab plus chemotherapy versus placebo plus chemotherapy in patients with HER2-negative, untreated, unresectable advanced or recurrent gastric or gastro-oesophageal junction cancer (ATTRACTION-4): a randomised, multicentre, double-blind, placebo-controlled, phase 3 trial, Lancet Oncol. 23 (2022) 234–247.
[6] A. Marabelle, D.T. Le, P.A. Ascierto, A.M. Di Giacomo, A.D. Jesus-Acosta, J.-P. Delord, et al., Efficacy of pembrolizumab in patients with noncolorectal high microsatellite instability/mismatch repair-deficient cancer: results from the Phase II KEYNOTE-158 study, J. Clin. Oncol. 38 (2020) 1–10.
[7] K. Shitara, M. Ozguroglu, Y.J. Bang, M.D. Bartolomeo, M. Mandala, M.-H. Ryu, et al., Pembrolizumab versus paclitaxel for previously treated, advanced gastric or gastro-oesophageal junction cancer (KEYNOTE-061): a randomised, open-label, controlled, phase 3 trial, Lancet 392 (2018) 123–133.
[8] M.A. Lancaster, J.A. Knoblich, Organogenesis in a dish: modeling development and disease using organoid technologies, Science 345 (2014), 1247125.
[9] T. Sato, D.E. Stange, M. Ferrante, R.G. Vries, J.H. Van Es, S. Van den Brink, et al., Long-term expansion of epithelial organoids from human colon, adenoma, adenocarcinoma, and Barrett's epithelium, Gastroenterology 141 (2011) 1762–1772.
[10] L. Broutier, G. Mastrogiovanni, M.M. Verstegen, H.E. Francies, L.M. Gavarró, C.R. Bradshaw, et al., Human primary liver cancer-derived organoid cultures for disease modeling and drug screening, Nat. Med. 23 (2017) 1424–1435.
[11] D. Gao, I. Vela, A. Sboner, P.J. Iaquinta, W.R. Karthaus, A. Gopalan, et al., Organoid cultures derived from patients with advanced prostate cancer, Cell 159 (2014) 176–187.
[12] S.F. Boj, C.I. Hwang, L.A. Baker, Chio II, D.D. Engle, V. Corbo, et al., Organoid models of human and mouse ductal pancreatic cancer, Cell 160 (2015) 324–338.
[13] H.H.N. Yan, H.C. Siu, S. Law, S.L. Ho, S.S.K. Yue, W.Y. Tsui, et al., A comprehensive human gastric cancer organoid biobank captures tumor subtype heterogeneity and enables therapeutic screening, Cell Stem Cell 23 (2018) 882–897.e11.
[14] N.G. Steele, J. Chakrabarti, J. Wang, J. Biesiada, L. Holokai, J. Chang, et al., An organoid-based preclinical model of human gastric cancer, Cell Mol. Gastroenterol. Hepatol. 7 (2019) 161–184.
[15] T. Seidlitz, S.R. Merker, A. Rothe, F. Zakrzewski, C. von Neubeck, K. Grützmann, et al., Human gastric cancer modelling using organoids, Gut 68 (2019) 207–217.
[16] N. Sachs, J. de Ligt, O. Kopper, E. Gogola, G. Bounova, F. Weeber, et al., A living biobank of breast cancer organoids captures disease heterogeneity, Cell 172 (2018) 373–386.e10.
[17] J.C.H. Kong, G.R. Guerra, R.M. Millen, S. Roth, H. Xu, P.J. Neeson, et al., Tumor-infiltrating lymphocyte function predicts response to neoadjuvant chemoradiotherapy in locally advanced rectal cancer, JCO Precis. Oncol. 2 (2018) 1–15.
[18] S. Ukai, R. Honma, N. Sakamoto, Y. Yamamoto, Q.T. Pham, K. Harada, et al., Molecular biological analysis of 5-FU-resistant gastric cancer organoids; KHDRBS3 contributes to the attainment of features of cancer stem cell, Oncogene 39 (2020) 7265–7278.
[19] K. Harada, N. Sakamoto, S. Ukai, Y. Yamamoto, Q.T. Pham, D. Taniyama, et al., Establishment of oxaliplatin-resistant gastric cancer organoids: importance of myoferlin in the acquisition of oxaliplatin resistance, Gastric Cancer 24 (2021) 1264–1277.
[20] K.K. Dijkstra, C.M. Cattaneo, F. Weeber, M. Chalabi, J. van de Haar, L.F. Fanchi, et al., Generation of tumor-reactive T cells by co-culture of peripheral blood lymphocytes and tumor organoids, Cell 174 (2018) 1586–1598.e12.
[21] J.G.C. Assoc, Japanese classification of gastric carcinoma: 3rd English edition, Gastric Cancer 14 (2011) 101–112.
[22] T. Nakano, S. Ando, N. Takata, M. Kawada, K. Muguruma, K. Sekiguchi, et al., Self-formation of optic cups and storable stratified neural retina from human ESCs, Cell Stem Cell 10 (2012) 771–785.